Nonreciprocity in Bianisotropic Systems with Uniform Time Modulation

X. Wang,[1,*] G. Ptitcyn,[1,*] V. S. Asadchy,[2,*] A. Díaz-Rubio,[1] M. S. Mirmoosa,[3]
Shanhui Fan,[2] and S. A. Tretyakov[1]
[1]Department of Electronics and Nanoengineering, Aalto University, P.O. Box 15500, FI-00076 Aalto, Finland
[2]Ginzton Laboratory and Department of Electrical Engineering, Stanford University, Stanford, California 94305, USA
[3]Laboratory of Wave Engineering, Swiss Federal Institute of Technology in Lausanne (EPFL), CH-1015 Lausanne, Switzerland

(Received 15 March 2020; accepted 12 October 2020; published 22 December 2020)

Physical systems with material properties modulated in time provide versatile routes for designing magnetless nonreciprocal devices. Traditionally, nonreciprocity in such systems is achieved exploiting both temporal and spatial modulations, which inevitably requires a series of time-modulated elements distributed in space. In this Letter, we introduce a concept of bianisotropic time-modulated systems capable of nonreciprocal wave propagation at the fundamental frequency and based on uniform, solely temporal material modulations. In the absence of temporal modulations, the considered bianisotropic systems are reciprocal. We theoretically explain the nonreciprocal effect by analyzing wave propagation in an unbounded bianisotropic time-modulated medium. The effect stems from temporal modulation of spatial dispersion effects which to date were not taken into account in previous studies based on the local-permittivity description. We propose a circuit design of a bianisotropic metasurface that can provide phase-insensitive isolation and unidirectional amplification.

DOI: 10.1103/PhysRevLett.125.266102

Reciprocity is a fundamental principle of a physical system, requiring that the transmission between two ports does not change if the source and receiver are interchanged. Breaking reciprocity is necessary for unidirectional wave propagation, such as wave isolation and circulation [1,2]. The conventional way for attaining nonreciprocity is to exert magnetic bias on magneto-optical materials [3,4], which, however, has a rather weak effect at high frequencies. Moreover, the devices based on magneto-optical materials are bulky and incompatible to systems where parasitic effects of external magnetic fields should be avoided. An alternative approach is to use nonlinear materials [5–8], but it only works for certain strengths of the incident signal and the functionalities are limited by the dynamic reciprocity constraint [9].

Dynamic modulation of the material properties brings an additional degree of freedom for obtaining unprecedented wave effects in acoustics [10,11], optics [12,13], and microwave engineering [14–16]. It was noticed quite early that an electronic device whose properties are modulated in space and in time can exhibit a nonreciprocal response [17–19]. In the last decade, due to advances in electronics and photonics, research interest in nonreciprocal wave propagation based on space-time modulated systems has rapidly revived and yielded various designs of nonreciprocal devices: isolators [20–24], circulators [25], phase shifters [26,27], and one-way amplifiers [28–30]. To date, all the known approaches for obtaining nonreciprocal wave propagation in time-modulated systems can be boiled down to the following three fundamental classes [31,32]: Traveling-wave modulators (indirect photonic transitions) [17,27,29,33–48], tandem phase modulators (and related approach based on direct photonic transitions) [22,49–53], and nonreciprocal frequency converters [54–56]. The first approach implies modulation of material properties in both space and in time, while the second requires two temporally modulated components separated in space. In both cases, it is necessary to use a series of time-modulated elements which have to be precisely synchronized with each other, which greatly increases the complexity of the biasing networks. The third approach requires either an asymmetric modulation function profile of the real part of permittivity [32,55] or modulating both its real and imaginary parts [54]. However, in both cases the system exhibits reciprocal transmission for the fundamental frequency since waves incident from the opposite directions "sense" effectively the same structure (nonreciprocity manifests itself only in nonreciprocal frequency conversion). Consequently, designing isolators using this frequency-converter approach requires cascading a pair of two converters, which results in additional device complexity [54,55].

In this Letter, we introduce a concept of linear bianisotropic time-modulated systems capable of nonreciprocal wave propagation at the fundamental frequency and implying solely temporal and uniform modulation of material properties. This route for nonreciprocal time-modulated systems, originated from bianisotropy (weak spatial dispersion), strikingly differs from the previously known three approaches based on the local-permittivity material description. It should be mentioned that in nonlinear systems, nonreciprocal response under uniform temporal modulation is possible by creating an external angular-momentum bias [57]. In addition to the fundamental theoretical importance, our approach additionally provides certain advantages for practical realization (it is sufficient to ensure temporal modulation of a single component in the nonreciprocal system). We explain and demonstrate the physics behind the new effect by analyzing wave propagation in an unbounded bianisotropic time-modulated medium (such a medium is reciprocal in the absence of temporal modulations). Next, we extend the study to two-dimensional bianisotropic metasurfaces (single-layer metamaterial composites). We design a deeply subwavelength metasurface that exhibits strong unidirectional transmission or unidirectional amplification. The metasurface incorporates a single temporally modulated capacitive layer backed by a usual dielectric layer. We show that the metasurface obeys the generalized time-reversal symmetry, but exhibits strong unidirectional amplification and attenuation. Finally, we propose an equivalent circuit for the bianisotropic metasurface capable of phase-insensitive isolation.

First, we analyze wave propagation in unbounded materials whose effective material parameters are modulated in time according to the same symmetric profile and with the same phase at each point in space (uniform or so-called global modulation). It will be shown that wave propagation in arbitrary anisotropic materials with global time modulation is always reciprocal. On the other hand, it will be shown that under the same conditions, reciprocity can be broken in bianisotropic materials.

The constitutive relations of a bulk bianisotropic material (reciprocal in the absence of temporal modulations) with antisymmetric magnetoelectric tensor (describing so-called omega magnetoelectric coupling) can be written in the form of [58] [Eq. (8.4)]

$$\mathbf{D} = \bar{\bar{\varepsilon}} \cdot \mathbf{E} + \Omega \bar{\bar{J}} \cdot \mathbf{H}, \qquad \mathbf{B} = \bar{\bar{\mu}} \cdot \mathbf{H} + \Omega \bar{\bar{J}} \cdot \mathbf{E}, \quad (1)$$

where $\bar{\bar{\varepsilon}}$ and $\bar{\bar{\mu}}$ are the anisotropic permittivity and permeability tensors, Ω is the amplitude of the bianisotropic omega coupling, and $\bar{\bar{J}} = \hat{\mathbf{z}} \times \bar{\bar{I}}$ is the transverse vector-product dyadic. Here, for simplicity, we use the adiabatic model for temporal modulations, assuming that the operational frequency ω is very low compared to the lowest resonance frequency of the material. In this case, the uniformly modulated material tensors can be written as (see Sec. 1 of the Supplemental Material [59]) $\bar{\bar{\varepsilon}}(\omega, t, \mathbf{r}) = \bar{\bar{\varepsilon}}_{\rm st}(\omega, \mathbf{r}) + \bar{\bar{M}}_{\varepsilon}(\mathbf{r}) \cos(\omega_m t + \phi)$, $\bar{\bar{\mu}}(\omega, t, \mathbf{r}) = \bar{\bar{\mu}}_{\rm st}(\omega, \mathbf{r}) + \bar{\bar{M}}_{\mu}(\mathbf{r}) \cos(\omega_m t + \phi)$, and $\Omega(\omega, t, \mathbf{r}) = M_{\Omega}(\mathbf{r}) \times \cos(\omega_m t + \phi)$, where $\bar{\bar{\varepsilon}}_{\rm st}$ and $\bar{\bar{\mu}}_{\rm st}$ denote static (in the absence of time modulation) permittivity and permeability, $\bar{\bar{M}}_{\varepsilon}$, $\bar{\bar{M}}_{\mu}$, and M_{Ω} are the modulation strength functions, ω_m is the modulation frequency, and ϕ is an arbitrary global phase. Note that this model can be used for arbitrary modulation frequency ω_m (see Sec. 1 of the Supplemental Material [59] for details). In the general nonadiabatic case, the following derivations could still be performed, writing the material parameters using integrals over past time.

Because of the periodical modulation, the electric and magnetic fields are written in terms of the Fourier components at frequencies $\omega_n = \omega_0 + n\omega_m$, i.e., $\mathbf{E}_n$ and $\mathbf{H}_n$. The external sources are characterized by the electric current harmonics $\mathbf{J}_{e,n}$, and time-harmonic oscillations in the form $e^{+j\omega t}$ are assumed. Analogously to derivations in Ref. [71], Eqs. (1) can be substituted into Maxwell equations and the wave equation can be written in the matrix form ([59], Sec. 2)

$$\begin{aligned} &-j(\{j[\omega]^{-1} \cdot [D] + [A_\Omega] \cdot [J]\} \cdot [A_\mu]^{-1} \\ &\quad \cdot \{j[\omega]^{-1} \cdot [D] - [A_\Omega] \cdot [J]\} + [A_\varepsilon]) \cdot [\mathbf{E}] = [\mathbf{J}'_e]. \quad (2) \end{aligned}$$

Here, $[\mathbf{E}]$ and $[\mathbf{J}'_e]$ denote the column vectors with components $\mathbf{E}_n$ and $\mathbf{J}'_{e,n} = \mathbf{J}_{e,n}/\omega_n$, and $[\omega]$ is the diagonal matrix with frequencies ω_n at the diagonal. Block matrix $[D]$ denotes vector operation $\nabla\times$ and block matrix $[J]$ is composed of antisymmetric matrices $\bar{\bar{J}}$ on the diagonal (see the definitions of the matrices in Sec. 2 of the Supplemental Material [59]). Block matrices $[A_\varepsilon]$, $[A_\mu]$, and $[A_\Omega]$ are described in Ref. [59] and include dependence on the modulation strength functions $\bar{\bar{M}}_{\varepsilon}$, $\bar{\bar{M}}_{\mu}$, and M_{Ω}, respectively. They can be made symmetric by selecting global phase $\phi = 0$ (the initial phase can be chosen arbitrarily by time translation $t \to t + \Delta t$). Equation (2) can be simplified to $[\mathbf{E}] = [G] \cdot [\mathbf{J}'_e]$ with $[G]$ being Green's function of the time-varying unbounded material written in the block matrix form. As shown in Sec. 2 of the Supplemental Material [59], the Green's function matrix of any anisotropic material (i.e., when $A_\Omega = 0$) is symmetric [22], which implies that wave propagation in such material is reciprocal and subject to the Lorentz reciprocity [2] [Eq. (119)]. On the contrary, an unbounded bianisotropic omega material with nonzero A_Ω breaks reciprocity since in this case matrix $[G]$ is always not symmetric. It should be noted that nonreciprocal transmission in bianisotropic material occurs even when permittivity and permeability are time invariant, i.e., $\bar{\bar{\varepsilon}}(\omega, t, \mathbf{r}) = \bar{\bar{\varepsilon}}_{\rm st}(\omega, \mathbf{r})$ and $\bar{\bar{\mu}}(\omega, t, \mathbf{r}) = \bar{\bar{\mu}}_{\rm st}(\omega, \mathbf{r})$. It is important to mention that nonreciprocity requires antisymmetric magnetoelectric coupling and cannot be achieved in isotropic chiral materials with globally modulated properties. This can be easily verified replacing $\Omega\bar{\bar{J}}$ in the former of Eq. (1) by $-\kappa\bar{\bar{I}}$ and the latter by $+\kappa\bar{\bar{I}}$ [58] [Eq. (8.4)].

The above derivations demonstrate that a bulk material with temporally modulated bianisotropic response supports nonreciprocal wave propagation. Since in most practical situations implementation of bulk bianisotropic materials can be complicated in terms of fabrication, next we consider the same effect in a two-dimensional single-layer array of bianisotropic elements (a metasurface).

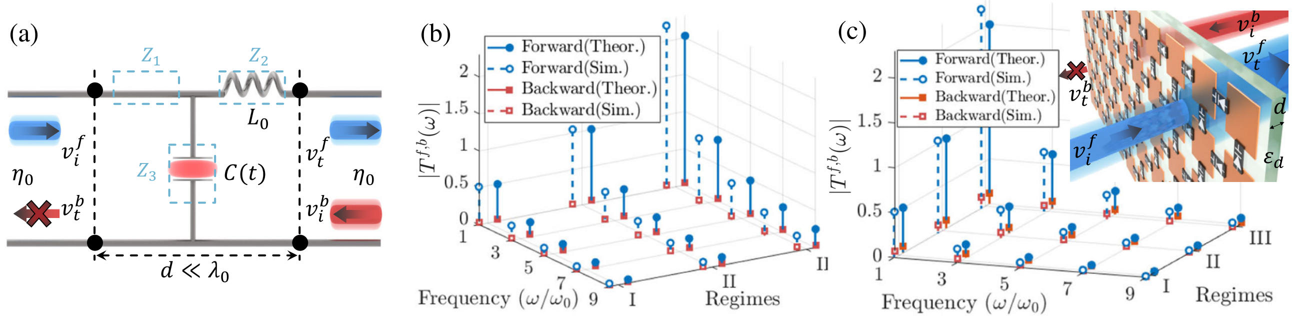

FIG. 1. (a) A T circuit that describes propagation of plane waves through a bianisotropic time-modulated metasurface. (b) Spectral response of the time-varying LC circuit for forward and backward incident waves. In all three regimes, $L_0 = 6.87$ nH, $\phi = 0$, and $A = 1$. The capacitances C_0 for the three regimes are $C_0 = 2.2$ pF for regime I, $C_0 = 1.6$ pF for regime II, and $C_0 = 1.55$ pF for regime III. The operating frequency is $f_0 = 10$ GHz. (c) The spectral response of the metasurface. Here, $C(t) = 6.8[1 - 0.9\sin(\omega_m t + 0.084\pi)]$ pF for regime I, $C(t) = 5.24[1 - 0.9\sin(\omega_m t + 1.131\pi)]$ pF for regime II, $C(t) = 4.12[1 - 0.9\sin(\omega_m t + 1.195\pi)]$ pF for regime III, $f_0 = 10$ GHz, $\epsilon_d = 65$, and $d = \lambda_0/30$.

Analogously to bulk materials which can be modeled by volume-averaged material parameters, metasurfaces are conventionally characterized by surface-averaged material parameters, i.e., polarizabilities, susceptibilities, or surface impedances ([72], Sec. 2.4). Thus, the above conclusions for time-varying bulk materials also apply to the time-modulated metasurfaces. In what follows, we choose the surface impedance model, which represents a metasurface as an equivalent circuit of specific configuration. Propagating plane waves with electric E and magnetic H fields are modeled by signals with voltages v and currents i propagating in an equivalent transmission line (Sec. 3 of the Supplemental Material [59]).

Any reciprocal bianisotropic metasurface can be described by an equivalent T or Π circuit. We model a metasurface with a T circuit formed by three lumped impedances in frequency domain, Z_1 and Z_2 connected in series and Z_3 connected in parallel, as shown in Fig. 1(a). The total thickness of the metasurface d can be deeply subwavelength. In such representation, the series impedances characterize effective magnetic polarization in the metasurface (due to possible induced circulating currents), while the parallel impedance corresponds to the electric polarization. The degree of asymmetry of the T circuit, proportional to the difference $Z_1 - Z_2$, characterizes the bianisotropic omega response [64] [related to the Ω parameter in Eq. (1) in the bulk material case]. Some possible conceptual realizations of bianisotropic omega-type metasurfaces are shown in Sec. 4 of the Supplemental Material [59].

As a proof of concept, here we consider the simplest circuit configuration that provides nonzero bianisotropic coupling. We choose the right series circuit element as an inductor with time-invariant inductance L_0, while the parallel element as a capacitor with temporally modulated capacitance $C(t) = C_0[1 - A\sin(\omega_m t + \phi)]$. The left series element is short circuited [see Fig. 1(a)]. Based on the time-domain analysis (Sec. 5 of the Supplemental Material [59]), the incident and transmitted voltages for forward and backward illuminations satisfy the following relations:

$$v_i^f(t) = \hat{P}(t)v_t^f(t), \quad v_i^b(t) = \left[\hat{P}(t) + \frac{L'}{2}\frac{d}{dt}\frac{dC'(t)}{dt}\right]v_t^b(t), \tag{3}$$

where operator $\hat{P}(t)$ is given by

$$\hat{P}(t) = 1 + \frac{1}{2}\frac{d}{dt}\left(C'(t) + L' + L'C'(t)\frac{d}{dt}\right). \tag{4}$$

Here, $v_i^{f,b}$ are the incident voltage signals (equivalent to incident electric fields) for the forward and backward illuminations, $L' = L_0/\eta_0$ and $C'(t) = \eta_0 C(t)$ are the inductance and capacitance normalized by the free-space wave impedance η_0 with the dimensions of time. As is seen from Eq. (3), the differential operators acting on transmitted voltages for the opposite illuminations $v_t^f(t)$ and $v_t^b(t)$ differ by the term which includes the time derivative of the capacitance function. Therefore, if $C'(t)$ is constant, both equations in Eq. (3) become identical, resulting in expected reciprocal propagation in the time-invariant metasurface. However, as will be shown below, a metasurface with nonzero $dC'(t)/dt$ in general can exhibit nonreciprocal transmission.

It is easy to test under what conditions the metasurface described by Eq. (3) exhibits nonreciprocal propagation at frequency ω_0. To do that, we choose modulation at $\omega_m = 2\omega_0$ (Sec. 5 of the Supplemental Material [59]). Such modulation frequency has been also applied, as examples, for wave amplification [17] and one-way beam splitting [48] but using space-time modulation schemes. Here, we assume the transmission signal for both incident directions is $v_t^{f,b} = \cos(\omega_0 t + \psi)$. In this way, the corresponding incident signals can be easily found by substituting $v_t^{f,b}$ into Eq. (3) ([59], Sec. 5). After knowing the incident fields,

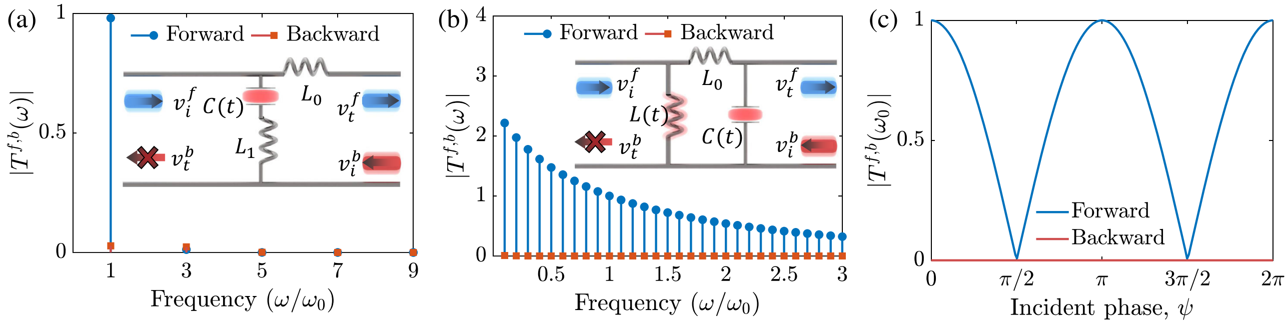

FIG. 2. (a) Spectral response of the modified circuit for small modulation amplitude. Here, $C(t) = 6.33[1 - 0.1\sin(2\omega_0 t)]$ fF, $L_0 = 6.2$ nH, and $L_1 = 38.2$ nH. (b) Spectral response of the modified circuit for reduced modulation frequency. Here, $L_0 = 216.1$ nH, $L(t) = 149.7[1 - \sin(0.1\omega_0 t)]$ nH, and $C(t) = 5.36[1 - \sin(0.1\omega_0 t)]$ pF. Isolation levels achieved at ω_0 is 68.1 dB. (c) Forward and backward transmission amplitudes of the fundamental harmonic as functions of the incident phase.

the transmission coefficients for forward and backward incidences at the fundamental frequency can be calculated as

$$T^f(\omega_0) = 4[Q - C_0 A\omega_0(\eta_0 - j\omega_0 L_0)e^{j(\phi-2\psi)}]^{-1}, \quad (5)$$

$$T^b(\omega_0) = 4[Q - C_0 A\omega_0(\eta_0 + j\omega_0 L_0)e^{j(\phi-2\psi)}]^{-1}, \quad (6)$$

where $Q = 4 - 2C_0 L_0 \omega_0^2 + 2j\omega_0(L' + C_0\eta_0)$. It is obvious that T^f and T^b are not equal only if $L_0 \neq 0$, which means that this structure is nonreciprocal only when bianisotropic coupling is present.

Interestingly, although the metasurface described by the circuit in Fig. 1(a) is nonreciprocal, it obeys the generalized time-reversal symmetry [32]. Under substitution $v(t) \to v(-t)$ and $\eta_0 \to -\eta_0$ (the latter substitution is due to the reversal of the current direction in the circuit, which is defined as $i(t) = v(t)/\eta_0$), relations (3) and (4) do not change their forms, providing that $C(t + \Delta t) = C(-t + \Delta t)$ for some specific gauge time translation Δt. Therefore, signal propagation in the circuit shown in Fig. 1(a) obeys the generalized time-reversal symmetry ([59], Sec. 6). Such nonreciprocal but time-reversal symmetric response was recently reported for static but non-Hermitian systems [73]. Our modulated system is also non-Hermitian, i.e., energy is not conserved in the system ([59], Sec. 10), and nonreciprocity manifests itself in terms of unidirectional amplification and attenuation.

The temporal modulation induces frequency mixing, and the reflected and transmitted signals contain infinite numbers of harmonics $\omega_n = \omega_0 + n\omega_m$, where n is an integer and refers to the harmonic order. In order to choose parameters L_0 and $C(t)$ of the circuit providing the highest nonreciprocity at the fundamental frequency, we optimize the circuit values based on the time-Floquet analysis (Sec. 7.1 of the Supplemental Material [59]) for given incident voltages $v_i^{f,b}(t) = \cos(\omega_0 t)$. In the numerical optimization using MATLAB, we define the cost function, $F = ||T^f(\omega_0)| - K| + |T^b(\omega_0)|$, and search for such a set of circuit parameters $\{L_0, C_0, A, \phi\}$ which ensures $F \to 0$ ([59], Sec. 9). Parameter K defines the desired transmission for the forward illumination, while for the backward illumination transmission should be always suppressed. We performed optimization of the circuit parameters for three different regimes: Forward-transmitted wave is attenuated by half (regime I: $K = 0.5$), unchanged (regime II: $K = 1$), and amplified (regime III: $K = 2$). The optimization results are shown and confirmed with the simulated results obtained from MathWorks Simulink in Fig. 1(b). The results demonstrate that the metasurface can perform one-way transmission by only modulating a single capacitor in the equivalent circuit, and the transmittance can be arbitrarily engineered with energy damping or amplification via modifying function $C(t)$. These features are very different from properties of the previously reported nonreciprocal devices [17,27,29,33–46]. All nonzero high-order frequency harmonics can be filtered out using a conventional frequency band-pass filter. The power and efficiency analyses of the system (also for the systems in Fig. 2) are presented in Sec. 10 of the Supplemental Material [59]. From Eqs. (5) and (6), it is obvious that the nonreciprocity level can be arbitrarily tuned by adjusting the value of static inductance (more details in Sec. 11 of the Supplemental Material [59]).

Next, we implement the designed time-modulated equivalent circuit [Fig. 1(a)] using a realistic metasurface structure performing nonreciprocal transmission or amplification for plane waves. The parallel capacitor in the circuit [Fig. 1(a)] can be implemented by an array of metallic patches, as shown in the inset of Fig. 1(c). Under plane wave incidence, the gaps between adjacent patches exhibit capacitive property. In each gap, we embed a varactor to tune the effective capacitance of the metasurface layer. By applying a time-harmonic voltage signal on the varactors, the effective capacitance of surface will change according to the function $C(t)$. The static inductance in the equivalent circuit can be implemented by a dielectric substrate. The required bianisotropic response of this metasurface is provided by its asymmetric geometry. Applying optimization based on the time-Floquet analysis ([59], Sec. 7.2), we find the optimal metasurface parameters for the three mentioned regimes [listed in the caption of Fig. 1(c)]. The transmission data through the metasurface is shown in Fig. 1(c). The results are similar to those in Fig. 1(b): the metasurface blocks transmission in the backward direction but allows transmission or amplification in the forward direction at ω_0.

The dynamic range of capacitance variations in the analyzed simple circuit example is relatively high, which can hinder practical implementations. Nevertheless, it can be significantly reduced by adding additional constant circuit elements to the considered circuit. In Fig. 2(a), we connect a static inductance to the time-varying capacitance in series and optimize the modulation function to realize an isolator ($K = 1$). The nonreciprocal effect is still evident even with the modulation amplitude as low as $A = 0.1$. Another issue is the high modulation speed ($\omega_m = 2\omega_0$), which can be easily realized in microwave frequencies but challenging in optics. However, it is important to note that in general, there is no fundamental restrictions for the choice of ω_m. Low speed modulation, such as $\omega_m = 0.1\omega_0$ and lower, can be achieved if the equivalent circuit comprises more than one modulated element (even having the same modulation law). Figure 2(b) shows that by adding a time-varying inductance $L(t)$ which is in-phase modulated with $C(t)$ (forming a Π-circuit), strong isolation ($K = 1$) can be achieved with the modulation frequency $\omega_m = 0.1\omega_0$. Importantly, as we change the phase of the incident wave, the backward transmission is always zero while the forward transmission changes along with the incident phase. This means that, if the pumping signal is synchronized with the forward incident signal (the synchronization mechanism is conceptually shown in Sec. 12 of the Supplemental Material [59]), the device can perform as a phase-insensitive isolator which can work even when illuminated simultaneously from both sides. The need for an additional time-varying circuit element does not mean that one should modulate more than one component in the actual metasurface. In general, the modulation of bianisotropic metasurfaces results in time dependence of all the circuit components in their equivalent circuits ([59], Sec. 4).

To summarize, we have introduced a concept of bianisotropic time-modulated systems capable of nonreciprocal wave propagation. In contrast to other approaches for nonreciprocal systems based on temporal modulations, our route provides high isolation (or amplification) at the fundamental frequency using only uniform temporal modulation of material properties. Our findings provide an attractive alternative for designing magnetless nonreciprocal microwave devices and, under a proper scheme of bianisotropic response in the metasurface, can be further extended to higher frequencies as well as applied to wave processes of a different nature.

This work was supported in part by the Academy of Finland (Project No. 309421), European Union's Horizon 2020 Future Emerging Technologies call (FETOPEN—RIA) under Grant No. 736876 (project VISORSURF), the Finnish Foundation for Technology Promotion, and the U.S. Air Force Office of Scientific Research MURI project (Grant No. FA9550-18-1-0379). The authors thank Dr. Momchil Minkov, Dr. Ian Williamson, Ms. Jiahui Wang, Professor Andrea Alù, and Dr. Robert Duggan for useful comments and discussions about the manuscript.

[*]These authors contributed equally.

[1] C. Caloz, A. Alù, S. Tretyakov, D. Sounas, K. Achouri, and Z.-L. Deck-Léger, Phys. Rev. Applied **10**, 047001 (2018).
[2] V. S. Asadchy, M. S. Mirmoosa, A. Daz-Rubio, S. Fan, and S. A. Tretyakov, Proc. IEEE **108**, 1684 (2020).
[3] Z. Wang and S. Fan, Appl. Phys. B **81**, 369 (2005).
[4] L. Bi, J. Hu, P. Jiang, D. H. Kim, G. F. Dionne, L. C. Kimerling, and C. Ross, Nat. Photonics **5**, 758 (2011).
[5] S. Lepri and G. Casati, Phys. Rev. Lett. **106**, 164101 (2011).
[6] M. Soljačić, C. Luo, J. D. Joannopoulos, and S. Fan, Opt. Lett. **28**, 637 (2003).
[7] I. V. Shadrivov, V. A. Fedotov, D. A. Powell, Y. S. Kivshar, and N. I. Zheludev, New J. Phys. **13**, 033025 (2011).
[8] L. Fan, J. Wang, L. T. Varghese, H. Shen, B. Niu, Y. Xuan, A. M. Weiner, and M. Qi, Science **335**, 447 (2012).
[9] Y. Shi, Z. Yu, and S. Fan, Nat. Photonics **9**, 388 (2015).
[10] R. Fleury, D. L. Sounas, C. F. Sieck, M. R. Haberman, and A. Alù, Science **343**, 516 (2014).
[11] G. Trainiti, Y. Ra'di, M. Ruzzene, and A. Alù, Sci. Adv. **5**, eaaw3255 (2019).
[12] D. L. Sounas and A. Alù, ACS Photonics **1**, 198 (2014).
[13] C. T. Phare, Y.-H. D. Lee, J. Cardenas, and M. Lipson, Nat. Photonics **9**, 511 (2015).
[14] N. A. Estep, D. L. Sounas, J. Soric, and A. Alù, Nat. Phys. **10**, 923 (2014).
[15] M. S. Mirmoosa, G. A. Ptitcyn, V. S. Asadchy, and S. A. Tretyakov, Phys. Rev. Appl. **11**, 014024 (2019).
[16] G. Ptitcyn, M. S. Mirmoosa, and S. A. Tretyakov, Phys. Rev. Res. **1**, 023014 (2019).
[17] A. Cullen, Nature (London) **181**, 332 (1958).
[18] A. K. Kamal, Proc. IRE **48**, 1424 (1960).
[19] J. Wentz, Proc. IEEE **54**, 97 (1966).
[20] S. Bhandare, S. K. Ibrahim, D. Sandel, H. Zhang, F. Wust, and R. Noé, IEEE J. Sel. Top. Quantum Electron. **11**, 417 (2005).
[21] Z. Yu and S. Fan, Nat. Photonics **3**, 91 (2009).
[22] K. Fang, Z. Yu, and S. Fan, Phys. Rev. Lett. **108**, 153901 (2012).
[23] H. Lira, Z. Yu, S. Fan, and M. Lipson, Phys. Rev. Lett. **109**, 033901 (2012).
[24] D. Correas-Serrano, J. Gomez-Diaz, D. Sounas, Y. Hadad, A. Alvarez-Melcon, and A. Alù, IEEE Antennas Wireless Propag. Lett. **15**, 1529 (2015).
[25] Y. Shi, S. Han, and S. Fan, ACS Photonics **4**, 1639 (2017).
[26] Z. Yu and S. Fan, Appl. Phys. Lett. **94**, 171116 (2009).
[27] X. Wang, A. Díaz-Rubio, H. Li, S. A. Tretyakov, and A. Alù, Phys. Rev. Appl. **13**, 044040 (2020).

[28] B. Abdo, K. Sliwa, L. Frunzio, and M. Devoret, Phys. Rev. X **3**, 031001 (2013).

[29] A. Y. Song, Y. Shi, Q. Lin, and S. Fan, Phys. Rev. A **99**, 013824 (2019).

[30] E. Galiffi, P. A. Huidobro, and J. B. Pendry, Phys. Rev. Lett. **123**, 206101 (2019).

[31] D. L. Sounas and A. Alù, Nat. Photonics **11**, 774 (2017).

[32] I. A. Williamson, M. Minkov, A. Dutt, J. Wang, A. Y. Song, and S. Fan, Proc. IEEE **108**, 1759 (2020).

[33] P. Dong, S. F. Preble, J. T. Robinson, S. Manipatruni, and M. Lipson, Phys. Rev. Lett. **100**, 033904 (2008).

[34] Z. Yu and S. Fan, Nat. Photonics **3**, 91 (2009).

[35] S. Qin, Q. Xu, and Y. E. Wang, IEEE Trans. Microwave Theory Tech. **62**, 2260 (2014).

[36] Y. Hadad, J. C. Soric, and A. Alù, Proc. Natl. Acad. Sci. U.S.A. **113**, 3471 (2016).

[37] S. Taravati and A. A. Kishk, IEEE Microw. Mag. **21**, 30 (2020).

[38] S. Taravati, N. Chamanara, and C. Caloz, Phys. Rev. B **96**, 165144 (2017).

[39] N. Chamanara, S. Taravati, Z.-L. Deck-Léger, and C. Caloz, Phys. Rev. B **96**, 155409 (2017).

[40] A. M. Shaltout, V. M. Shalaev, and M. L. Brongersma, Science **364**, eaat3100 (2019).

[41] A. M. Shaltout, A. Kildishev, and V. Shalaev, Opt. Mater. Express **5**, 2459 (2015).

[42] A. E. Cardin, S. R. Silva, S. R. Vardeny, W. J. Padilla, A. Saxena, A. J. Taylor, W. J. Kort-Kamp, H.-T. Chen, D. A. Dalvit, and A. K. Azad, Nat. Commun. **11**, 1469 (2020).

[43] L. Zhang, X. Q. Chen, R. W. Shao, J. Y. Dai, Q. Cheng, G. Castaldi, V. Galdi, and T. J. Cui, Adv. Mater. **31**, 1904069 (2019).

[44] A. Li, Y. Li, J. Long, E. Forati, Z. Du, and D. Sievenpiper, Opt. Lett. **45**, 1212 (2020).

[45] S. Taravati and G. V. Eleftheriades, Phys. Rev. Appl. **12**, 024026 (2019).

[46] D. Ramaccia, D. L. Sounas, A. Alù, F. Bilotti, and A. Toscano, IEEE Antennas Wireless Propag. Lett. **17**, 1968 (2018).

[47] S. Taravati, Phys. Rev. B **96**, 235150 (2017).

[48] S. Taravati and A. A. Kishk, Phys. Rev. B **99**, 075101 (2019).

[49] C. R. Doerr, N. Dupuis, and L. Zhang, Opt. Lett. **36**, 4293 (2011).

[50] C. Galland, R. Ding, N. C. Harris, T. Baehr-Jones, and M. Hochberg, Opt. Express **21**, 14500 (2013).

[51] L. Baldwin, Proc. Inst. Radio Eng. **49**, 1075 (1961).

[52] J. Hamasaki, Bell Syst. Tech. J. **43**, 1123 (1964).

[53] H. Brenner, IEEE Trans. Microwave Theory Tech. **15**, 301 (1967).

[54] T. T. Koutserimpas and R. Fleury, Phys. Rev. Lett. **120**, 087401 (2018).

[55] Z. Wu and A. Grbic, IEEE Trans. Antennas Propag. **68**, 1599 (2020).

[56] H. B. Henning, IEEE Trans. Broadcast Telev. Receivers **BTR-10**, 55 (1964).

[57] R. Duggan, D. Sounas, and A. Alù, Optica **6**, 1152 (2019).

[58] A. Serdyukov, I. Semchenko, S. Tretyakov, and A. Sihvola, in *Electromagnetics of Bi-Anisotropic Materials—Theory and Application*, Vol. 11 (Gordon and Breach Science Publishers, Amsterdam, 2001), p. 131.

[59] See Supplemental Material at http://link.aps.org/supplemental/10.1103/PhysRevLett.125.266102 for additional information, which includes Refs. [60–70].

[60] S. Ohler, B. Gilchrist, and A. Gallimore, IEEE Trans. Plasma Sci. **27**, 587 (1999).

[61] M. S. Mirmoosa, T. T. Koutserimpas, G. A. Ptitcyn, S. A. Tretyakov, and R. Fleury, arXiv:2002.12297.

[62] F. Martin, *Artificial Transmission Lines for RF and Microwave Applications* (John Wiley & Sons, New York, 2015).

[63] Y. Ra'di, V. S. Asadchy, and S. A. Tretyakov, IEEE Trans. Antennas Propag. **62**, 3749 (2014).

[64] M. Yazdi, M. Albooyeh, R. Alaee, V. Asadchy, N. Komjani, C. Rockstuhl, C. R. Simovski, and S. Tretyakov, IEEE Trans. Antennas Propag. **63**, 3004 (2015).

[65] R. Alaee, M. Albooyeh, A. Rahimzadegan, M. S. Mirmoosa, Y. S. Kivshar, and C. Rockstuhl, Phys. Rev. B **92**, 245130 (2015).

[66] A. Slobozhanyuk, S. H. Mousavi, X. Ni, D. Smirnova, Y. S. Kivshar, and A. B. Khanikaev, Nat. Photonics **11**, 130 (2017).

[67] S. Y. Elnaggar and G. N. Milford, IEEE Trans. Antennas Propag. **68**, 6636 (2020).

[68] J. Li, X. Zhu, C. Shen, X. Peng, and S. A. Cummer, Phys. Rev. B **100**, 144311 (2019).

[69] S. Tretyakov, *Analytical Modeling in Applied Electromagnetics* (Artech House, Boston, 2003).

[70] D. M. Pozar, *Microwave Engineering* (John Wiley & Sons, New York, 2012).

[71] Y. Shi, W. Shin, and S. Fan, Optica **3**, 1256 (2016).

[72] *Surface Electromagnetics: With Applications in Antenna, Microwave, and Optical Engineering*, edited by F. Yang and Y. Rahmat-Samii (Cambridge University Press, Cambridge, England, 2019).

[73] S. Buddhiraju, A. Song, G. T. Papadakis, and S. Fan, Phys. Rev. Lett. **124**, 257403 (2020).